TRENDS IN SCIENCES 2026; 23(10): 13267
https://doi.org/10.48048/tis.2026.13267 RESEARCH ARTICLE

Neuroprotective Potential of p-MCA in *Drosophila*

Nur Rahma Rumata[1,2], Asbah Asbah[3,8], Nadila Pratiwi Latada[8], Muhammad Arfandy Gunawan[4], Fifi Dismayanti Indriani Nainu[5], Irmanida Batubara[6], Muhammad Aswad[7], Berry Juliandi[1,*] and Firzan Nainu[3,8]

[1]*Department of Biology, Faculty of Mathematics and Natural Sciences, IPB University, Bogor 16680, Indonesia*
[2]*Faculty of Health Sciences, Almarisah Madani University, Makassar 90245, Indonesia*
[3]*Department of Pharmacy, Faculty of Pharmacy, Hasanuddin University, Makassar 90245, Indonesia*
[4]*Postgraduate Program in Faculty of Pharmacy, Hasanuddin University, Makassar 90245, Indonesia*
[5]*Postgraduate Program in Biomedical Sciences, Postgraduate Program, Hasanuddin University, Makassar 90245, Indonesia*
[6]*Department of Chemistry, Faculty of Mathematics and Natural Sciences, Tropical Biopharmaca Research Center - IPB University, Bogor 16680, Indonesia*
[7]*Faculty of Pharmacy, Hasanuddin University, Makassar 90245, Indonesia*
[8]*Unhas Fly Research Group, Faculty of Pharmacy, Hasanuddin University, Makassar 90245, Indonesia*

([*]Corresponding author's e-mail: bjuliandi@apps.ipb.ac.id)

Received: 5 January 2026, Revised: 21 February 2026, Accepted: 1 March 2026, Published: 10 May 2026

Abstract

p-methoxycinnamic acid (p-MCA), a bioactive compound from *Kaempferia galanga*, was evaluated for its neuroprotective effects in an Alzheimer's disease (AD)-like model of *Drosophila melanogaster*, supported by *in silico* docking and molecular dynamics simulations. Toxicity screening identified 10 mM $AlCl_3$ (aluminium chloride) as an effective concentration to induce neurodegenerative phenotypes without excessive mortality. p-MCA (0.01-0.1 mM) significantly improved survival, locomotor performance, and phototactic responses in $AlCl_3$-exposed flies. Gene expression analysis showed upregulation of antioxidant *(sod1, hsp22)* and anti-aging *(srl)* genes, along with modulation of the apoptosis-related gene *grim*, indicating regulation of oxidative stress and cellular homeostasis. Computational analysis demonstrated stable binding of p-MCA to acetylcholinesterase (ΔG = –7.2 kcal/mol), comparable to 10-40. Collectively, these findings indicate that p-MCA mitigates $AlCl_3$-induced neurotoxicity through multi-target mechanisms and supports its further evaluation in neurodegenerative disease models.

Keywords: p-MCA, Alzheimer's disease, Neuroprotection, *D. melanogaster*, Oxidative stress, Drug discovery, Neurodegenerative disorders

Introduction

Aging is associated with progressive functional decline driven by oxidative stress, genomic instability, and cellular damage, increasing the risk of neurodegenerative diseases such as Alzheimer's disease (AD) [1,2]. AD is characterized by central nervous system degeneration, amyloid beta (Aβ) plaque deposition, and neurofibrillary tangles, leading to synaptic dysfunction and cognitive decline [3-7]. As the most prevalent age-related neurodegenerative disorder, AD represents a major global health concern, particularly in aging populations, including Indonesia, where cases are projected to rise substantially by 2030 [8].

Current pharmacological treatments, such as N-methyl-D-aspartate receptor antagonists (memantine) and cholinesterase inhibitors, provide only symptomatic relief without preventing disease progression [3,9-12]. These limitations highlight the need for multi-target

therapeutic strategies addressing the molecular mechanisms underlying AD pathology [4,11].

Natural compounds have gained attention as potential neuroprotective agents. p-MCA derived from *Kaempferia galanga* exhibits antimicrobial, anticancer, anti-inflammatory, and anticholinesterase activities [12,13]. Experimental evidence indicates that p-MCA protects neurons from excitotoxicity and attenuates memory impairment in animal models, suggesting neuroprotective potential. However, its underlying molecular and genetic mechanisms remain insufficiently characterized.

Drosophila melanogaster provides a cost-effective and genetically tractable *in vivo* model for aging and neurodegeneration research [14-16], sharing substantial genetic conservation with humans and supporting transgenic approaches for mechanistic studies and therapeutic screening [16-18]. Therefore, this study aims to evaluate the neuroprotective effects of p-MCA using *D. melanogaster* as an AD-like model, providing mechanistic insights relevant to the development of novel therapeutic strategies for neurodegenerative diseases.

Materials and methods

This preclinical experimental study used a post-test only control design to evaluate the neuroprotective effects of p-MCA against $AlCl_3$-induced AD-like pathology in *D. melanogaster* (w^{1118}). Behavioral assays (toxicity, survival, locomotor activity, and phototaxis), gene expression analysis, and *in silico* molecular studies were conducted.

D. melanogaster stock

Adult male and female *D. melanogaster* (w^{1118}) were used in this study. The fly line was obtained from the Laboratory of Host Defense and Responses, Kanazawa University, Japan, and maintained for more than 20 generations in the Laboratory of Pharmacology and Toxicology, Faculty of Pharmacy, Universitas Hasanuddin, Indonesia. Flies were reared on a standard cornmeal-based medium at 25 °C under a 12-hour light/dark cycle [19].

Sample preparation

p-MCA, obtained from Tokyo Chemical Industry Co. Ltd®, was dissolved in analytical-grade dimethyl sulfoxide (DMSO).

Toxicity assay

To determine a non-lethal concentration of $AlCl_3$ for AD-like induction, a toxicity assay was performed. w^{1118} flies (3-5 day-old, 10 flies per vial) were exposed to $AlCl_3$ at concentrations of 10, 20, 30, and 40 mM for 7 days, with three replicates per group. Flies were maintained at 25 °C, and survival was recorded daily. $AlCl_3$ was dissolved in distilled water and administered via the fly medium.

Survival assay

Survival analysis was conducted using 3-5 day-old w^{1118} flies (5 males and 5 females per vial). Flies were treated with p-MCA at concentrations of 1, 0.1, 0.01, or 0.001 mM in combination with $AlCl_3$, while the control group received standard diet. Food was replaced every two days, and survival was recorded daily for 7 days. Survival data were analyzed using Kaplan-Meier curves with log-rank tests in GraphPad Prism® 8. An initial dose-range screening (1, 0.1, 0.01, and 0.001 mM) was performed in survival and locomotor assays to assess the toxicity and biological responsiveness of p-MCA under $AlCl_3$ exposure. Concentrations showing non-lethal profiles and measurable protective effects were subsequently selected for downstream molecular and behavioral analyses.

Negative geotaxis and phototaxis assays

Locomotor and sensory-cognitive functions were assessed using negative geotaxis and phototaxis assays, respectively. Negative geotaxis was performed with minor modifications of a previously described protocol [26], in which treated flies (3-5 day-old) were transferred into vertically oriented vials marked with a reference line, tapped to the bottom, and the number of flies crossing the line within 15 seconds was recorded. Flies treated with $AlCl_3$ (10 mM) and p-MCA for 7 days were analyzed. Phototactic behavior was evaluated as an indicator of sensory and cognitive function [20,21]. For this assay, 0.01 mM was selected based on preliminary screening demonstrating consistent efficacy without toxicity. Thirty age-matched flies per group (30 males

and 30 females analyzed separately) were randomly selected and tested. After 30 min of dark adaptation, flies were placed in a horizontally positioned phototaxis apparatus perpendicular to a light source (15 cm distance). The apparatus was divided into four sections, and fly distribution was recorded at 1-min intervals. Each assay included three consecutive technical trials using the same flies and vial on the same day, and the mean value was used for statistical analysis. Control measurements were performed using an identical apparatus aligned parallel to the light source. Results were expressed as the percentage of flies in the light and dark compartments.

Gene expression assay

Based on the survival screening results, 1, 0.1, and 0.01 mM were selected for gene expression analysis. The highest concentration (1 mM) was included to evaluate potential upper-range molecular responses, while 0.1 and 0.01 mM were selected due to their survival-prolonging effects. The lowest concentration (0.001 mM) was excluded from further mechanistic assays due to the absence of detectable biological effects in the initial screening. Total RNA was isolated from five live flies per experimental group using the Monarch Total RNA Miniprep Kit (New England Biolabs, Inc., MA). RNA concentration was measured using a NanoDrop spectrophotometer (BioDrop, USA). Expression levels of *sod1, hsp22, rpr, grim, srl*, and AChE were quantified by RT-qPCR using Luna® reagents (New England Biolabs, Inc., MA, USA) in a 10 µL reaction volume. The *rp49* gene was used as an internal reference. Amplification was performed using a Rotor-Gene Q thermal cycler (Qiagen, Germany) under standard cycling conditions, followed by melt curve analysis. Relative gene expression was calculated using comparative quantification. Primer sequences are listed in **Table 1** [22].

Table 1 Primers used in the RT-qPCR assay.

Genes	Forward primer	Reverse primer
sod1	5'– AGG TCA ACA TCA CCG ACT CC – 3'	5'– GTT GAC TTG CTC AGC TCG TG – 3'
hsp22	5' – TAC AAT GCG TTT CCT TAC CGA – 3'	5' – CAA TCT GCT GCC AGT TCC T – 3'
grim	5' –TCG GAG TTT GGA TGC TGG GAT CTT– 3'	5' – AGT CAC GTC GTC CTC ATC GTT GTT – 3'
srl	5' – CTC TTG GAG TCC GAG ATC CG CAA – 3'	5' – GGG ACC GCG AGC TGA TGG TT – 3'
AChE	5' – GCC GTG GGC AAT GTA ATA GT – 3'	5'– CGA CTC TCC GAA CAG TGT CA – 3'
rp49	5' – GAC GCT TCA AGG GAC AGT ATC TG – 3'	5' – AAA CGC GGT TCT GCA TGA G – 3'

Molecular docking and molecular dynamics

The 3D structures of p-MCA (CID: 699414) and 10-40 (CID: 3152) were retrieved from PubChem and prepared using UCSF Chimera® [23,24]. Docking validation was carried out by re-docking the native ligand and calculating RMSD values using PyMOL, with interaction visualization performed in Discovery Studio® [24,25]. Molecular dynamics simulations were conducted using YASARA with the Amber14 force field. Simulations were run for 100 ns at 310 K and pH 7.4 under periodic boundary conditions. RMSD, RMSF, and radius of gyration were analyzed at 2.5 ps intervals [26].

Data processing

Survival data were analyzed using Kaplan-Meier curves and log-rank tests. Locomotor, phototaxis, and gene expression data were analyzed by one-way ANOVA followed by Tukey's HSD post hoc test. Data are presented as mean ± SD, and $p < 0.05$ was considered statistically significant. Statistical analyses were performed using GraphPad Prism® 8.

Results and discussion

Dose-dependent toxicity of $AlCl_3$ in *D. melanogaster*

This study aimed to determine the lowest effective dose of $AlCl_3$ that induces Alzheimer's-like symptoms without causing excessive toxicity. Exposure to $AlCl_3$ for 7 days resulted in a concentration-dependent reduction in survival of *D. melanogaster*. Flies treated with 10-40 mM $AlCl_3$ exhibited progressively decreased survival compared to the untreated control (**Figure 1**), indicating increasing toxicity at higher concentrations. Among the tested doses, 10 mM $AlCl_3$-induced measurable neurodegenerative stress without causing excessive mortality and was therefore selected for subsequent experiments as an AD-like induction dose.

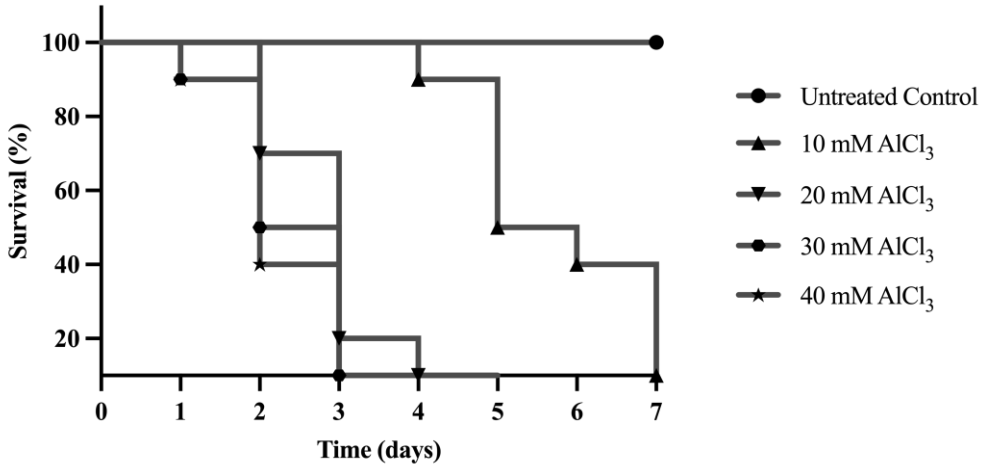

Figure 1 Dose-dependent toxicity of $AlCl_3$ as an inducer for neurodegeneration in *D. melanogaster*. The survival of *D. melanogaster* declined upon exposure to different concentrations of $AlCl_3$ (10-40 mM) compared to untreated control group. Since $AlCl_3$ was dissolved in distilled water, the untreated control group served as the appropriate control condition.

p-MCA enhances survival in *D. melanogaster* exposed to $AlCl_3$

This study investigated the neuroprotective effects of p-MCA by assessing its impact on the lifespan of *D. melanogaster* treated with $AlCl_3$. Administration of p-MCA significantly improved survival in flies exposed to 10 mM $AlCl_3$ (**Figure 2**). Notably, p-MCA at 0.1 mM and 0.01 mM produced the most pronounced effects, whereas higher and lower concentrations showed limited benefit. These findings indicate a concentration-dependent protective effect of p-MCA, consistent with its reported antioxidant and cytoprotective properties. Improved survival suggests that p-MCA enhances cellular resilience against $AlCl_3$-induced toxicity, a key feature relevant to neurodegenerative pathology.

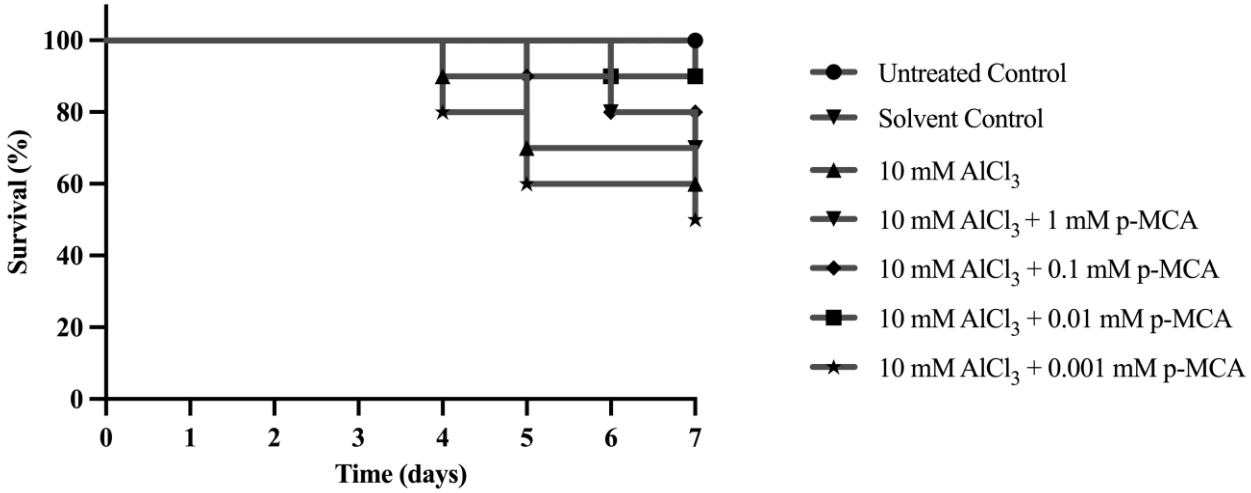

Figure 2 Improvement of *D. melanogaster* survival after administration of 10 mM $AlCl_3$ and p-MCA at various concentrations (1 mM, 0.1 mM, 0.01 mM, and 0.001 mM). Flies were treated with 10 mM $AlCl_3$ prior to treatment with p-MCA.

p-MCA enhances locomotor and cognitive function in *D. melanogaster* exposed to $AlCl_3$

Negative geotaxis analysis revealed that exposure to $AlCl_3$ significantly impaired locomotor activity in adult *D. melanogaster*. In contrast, p-MCA treatment markedly improved climbing performance across the tested concentrations, indicating attenuation of $AlCl_3$-induced motor dysfunction (**Figure 3(A)**).

Phototaxis assays further demonstrated that p-MCA preserved light-directed behavior in both male and female flies. Male flies treated with p-MCA showed a significantly higher proportion migrating toward the light source compared to the $AlCl_3$ only group (**Figure 3(B)**). A similar protective effect was observed in female flies, where p-MCA treatment restored phototactic responses disrupted by $AlCl_3$ exposure (**Figure 3(C)**). Together, these behavioral outcomes support the neuroprotective role of p-MCA in maintaining motor coordination and sensory-cognitive function under neurotoxic stress.

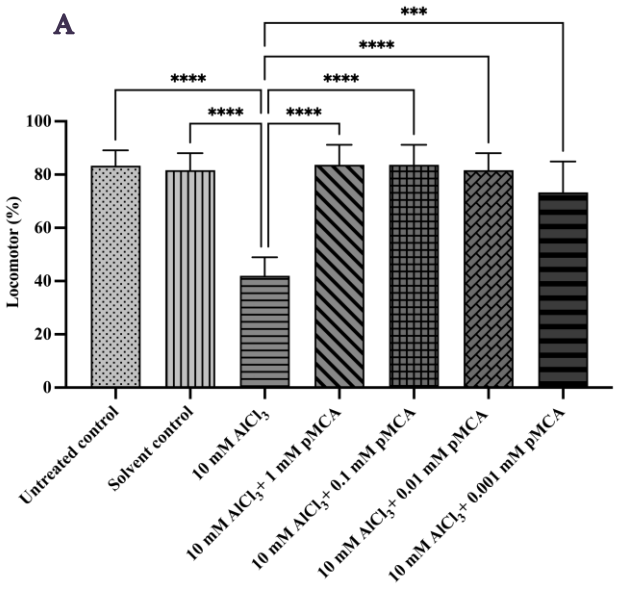

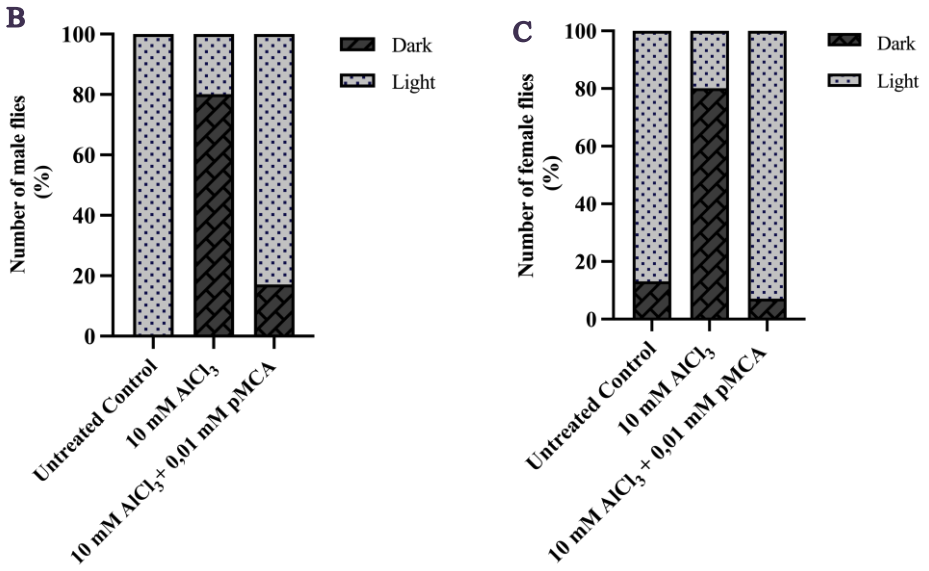

Figure 3 Improvement of locomotor activity (A) and phototaxis response in male (B) and female (C) adult *D. melanogaster* w^{1118} following exposure to 10 mM $AlCl_3$ and p-MCA at various concentrations (locomotor assay, A) and at 0.01 mM p-MCA (phototaxis assay, B - C). Data are expressed as mean ± SD. ***$p < 0.001$ and ****$p < 0.0001$ compared with the $AlCl_3$-treated group.

p-MCA modulates gene expression of *D. melanogaster* exposed to $AlCl_3$

RT-qPCR analysis demonstrated that p-MCA significantly modulated the expression of genes associated with antioxidant defense and stress response in $AlCl_3$-exposed *D. melanogaster*. *sod1* expression was significantly upregulated at 0.01 mM p-MCA compared with the $AlCl_3$ group (**Figure 4(A)**). Conversely, *hsp22* expression was consistently downregulated across all p-MCA concentrations (1, 0.1, and 0.01 mM) relative to $AlCl_3$ exposure alone (**Figure 4(B)**).

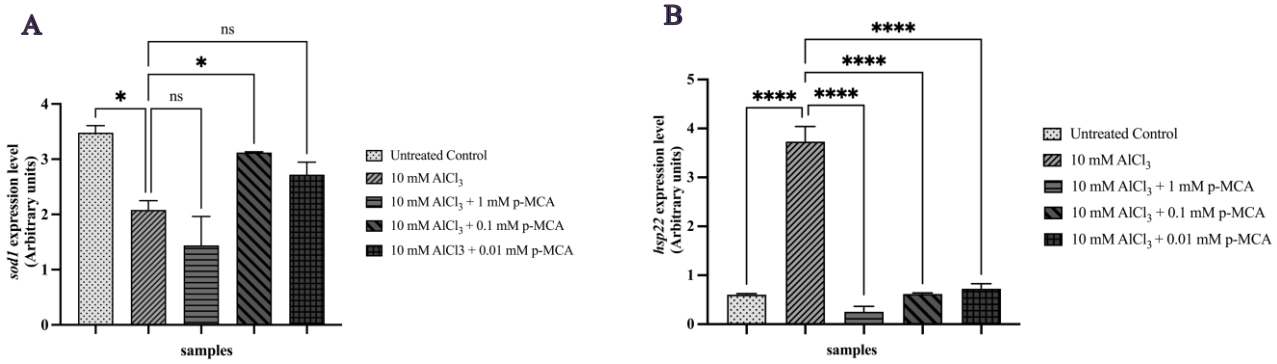

Figure 4 Relative expression levels of *sod1* (A) and *hsp22* (B) genes in adult *D. melanogaster* w^{1118} following exposure to 10 mM $AlCl_3$ and p-MCA at different concentrations, as determined by RT-qPCR and normalized to *rp49*. Data are presented as mean ± SD. *$p < 0.05$ and ****$p < 0.0001$ compared with the $AlCl_3$-treated group; ns, not significant.

Expression of the apoptosis-related gene *grim* was significantly increased at 0.01 mM p-MCA compared with the $AlCl_3$ group (**Figure 5(A)**). In parallel, the anti-aging gene srl showed significant upregulation at 0.1 and 0.01 mM p-MCA (**Figure 5(B)**).

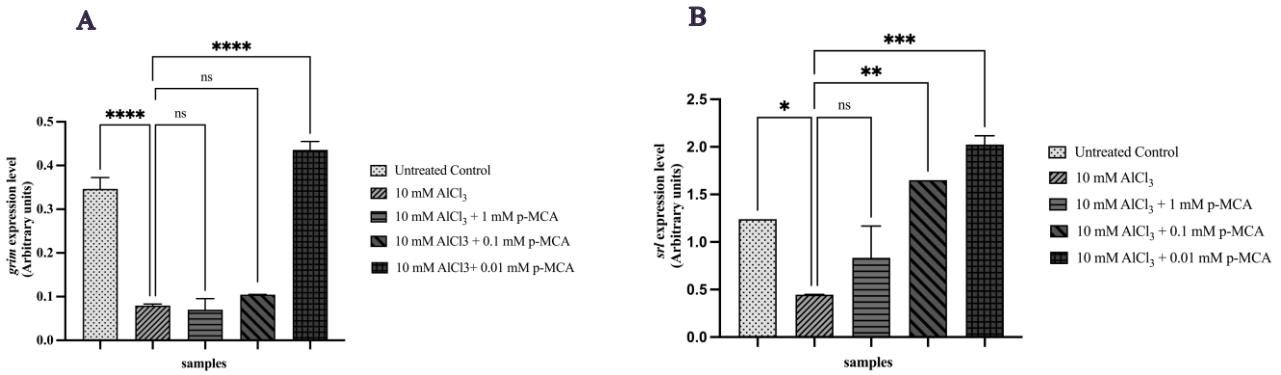

Figure 5 Relative expression levels of *grim* (A) and *srl* (B) genes in adult *D. melanogaster* w^{1118} following exposure to 10 mM $AlCl_3$ and p-MCA at different concentrations, as determined by RT-qPCR and normalized to *rp49*. Data are presented as mean ± SD. *$p < 0.05$, **$p < 0.01$, ***$p < 0.001$, and ****$p < 0.0001$ compared with the $AlCl_3$-treated group; ns, not significant.

Expression of AChE was significantly increased in flies treated with p-MCA at 0.01 mM compared with the $AlCl_3$ group (**Figure 6**). As AChE regulates acetylcholine turnover, this change may reflect compensatory regulation of cholinergic signaling in response to $AlCl_3$-induced neurotoxicity. However, interpretation of AChE expression requires caution due to the use of whole-body RNA extracts, which may include non-neuronal contributions.

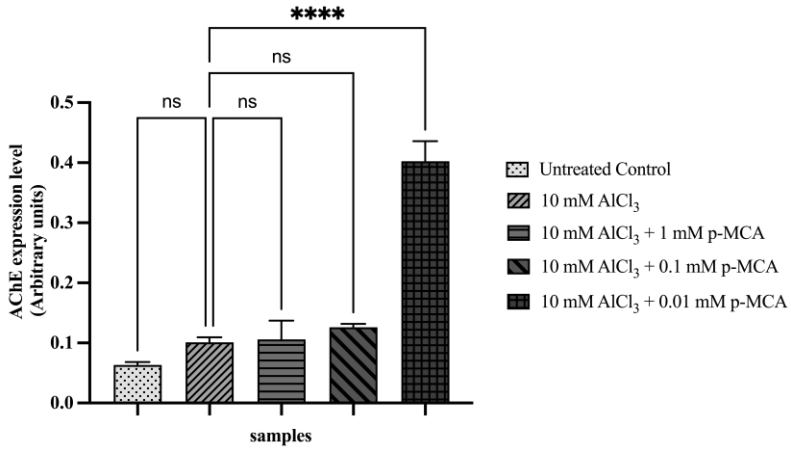

Figure 6 Relative expression level of AChE in adult *D. melanogaster* w^{1118} following exposure to 10 mM $AlCl_3$ and p-MCA at different concentrations, as determined by RT-qPCR and normalized to *rp49*. Data are presented as mean ± SD. ****$p < 0.0001$ compared with the $AlCl_3$-treated group; ns, not significant.

Molecular docking analysis demonstrated that p-MCA binds to *D. melanogaster* AChE with a binding free energy of –7.8 kcal/mol (**Figure 7(A)**), indicating moderate affinity compared to 10-40 (–9.5 kcal/mol). p-MCA interacted with key residues within the catalytic site, supporting its inhibitory potential. Molecular dynamics simulations further revealed stable ligand-protein interactions, with RMSD and radius of gyration profiles comparable to 10-40 (**Figure 7(B)**).

A

Compound	Acetylcholinesterase for *Drosophilla* (6XYU)	
	ΔG	**Hydrogen Bond**
trans-4-methoxycinnamic acid	-7.8	Glu80
Donepezil	-9.5	-

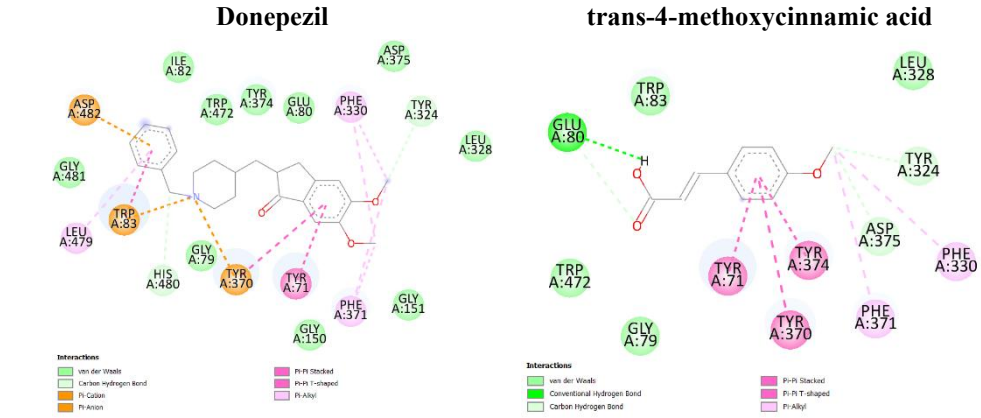

B

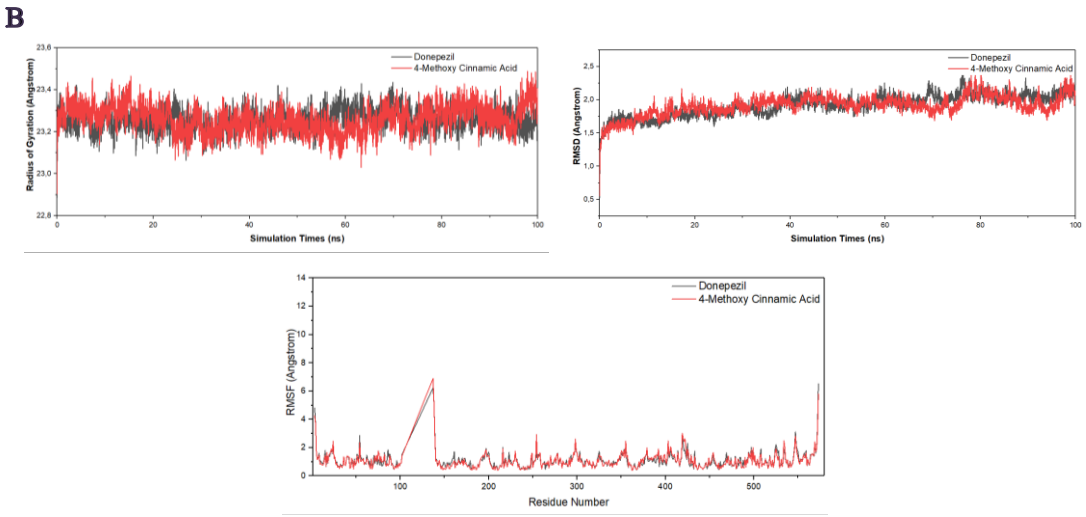

Figure 7 Results of molecular docking (A) and molecular dynamics (B) of acetylcholinesterase inhibitor in *D. melanogaster*.

Docking and simulation analyses were focused on AChE due to the established relevance of cholinergic dysfunction in AD and the availability of validated computational protocols. This targeted approach enabled direct correlation between molecular interactions and observed behavioral outcomes.

Docking studies using human AChE confirmed that p-MCA interacts with conserved residues, including Phe295, Tyr337, and Trp86, with a binding free energy

of −7.2 kcal/mol (**Figure 8(A)**). Molecular dynamics simulations showed stable interaction profiles comparable to 10-40, as indicated by RMSD, RMSF, and radius of gyration analyses (**Figure 8(B)**). These findings suggest that p-MCA exhibits conserved inhibitory behavior across species.

A

Compound	Acetylcholinesterase (4EY7)	
	ΔG	Hydrogen Bond
trans-4-methoxycinnamic acid	-7.2	Phe295
Donepezil	-12.2	Phe295

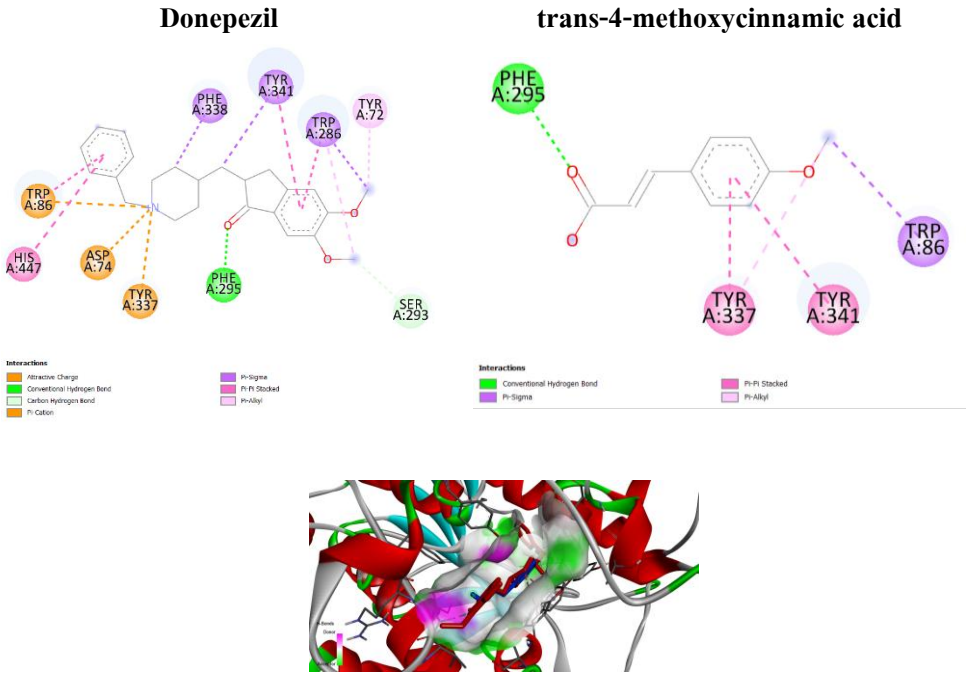

B

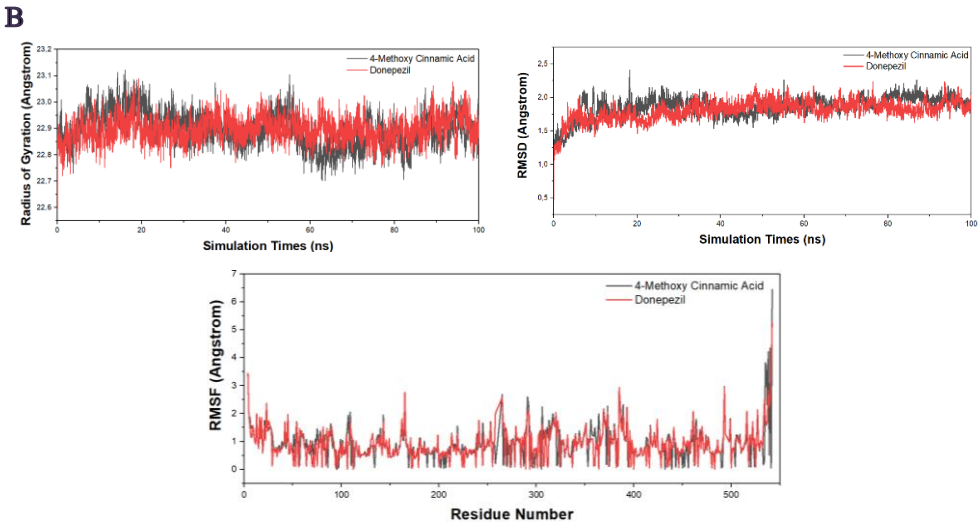

Figure 8 Results of molecular docking (A) and molecular dynamics (B) of acetylcholinesterase inhibitor in *Homo sapiens*.

p-MCA, a cinnamic acid derivative, has been reported to exert neuroprotective effects through antioxidant, anti-inflammatory, and apoptosis-regulating mechanisms [34,35]. In this study, its neuroprotective potential was evaluated using an integrated *in vivo* and *in silico* approach in *D. melanogaster* as a model of Alzheimer's disease (AD)-like neurodegeneration. $AlCl_3$ exposure reduced survival and impaired locomotor and cognitive performance, consistent with aluminum-induced neurotoxicity. A concentration of 10 mM produced clear neurodegenerative phenotypes without excessive mortality, providing a stable model. p-MCA, particularly at 0.01 and 0.1 mM, significantly improved survival and behavioral performance, indicating protection against oxidative and cellular damage associated with AD pathology [12,27].

Behavioral improvements in negative geotaxis and phototaxis further confirmed preservation of motor and sensory-cognitive functions, both established indicators of neurodegeneration in *Drosophila*. Dose selection for mechanistic assays was guided by preliminary survival screening to ensure biologically active yet non-toxic concentrations. At the molecular level, p-MCA modulated genes involved in oxidative stress, mitochondrial function, apoptosis, and aging. Upregulation of *sod1* suggests enhanced antioxidant capacity and improved redox homeostasis, which is critical given neuronal vulnerability to reactive oxygen species (ROS) and mitochondrial dysfunction in AD [28,29].

Increased expression of *srl,* the *Drosophila* homolog of PGC-1α, supports improved mitochondrial biogenesis and bioenergetic resilience under neurotoxic stress [30]. In contrast, reduced *hsp22* expression likely reflects attenuation of mitochondrial stress rather than diminished protection [31], consistent with concurrent *sod1* and *srl* upregulation. Upregulation of the pro-apoptotic gene *grim* indicates modulation of apoptosis-related pathways. In *Drosophila*, apoptotic signaling can occur in a regulated, context-dependent manner to eliminate damaged cells without widespread degeneration [32]. Thus, *grim* induction may represent adaptive cellular regulation rather than pathological neurodegeneration.

Although acetylcholinesterase (AChE) expression increased in some groups, molecular docking and dynamics simulations demonstrated stable binding of p-MCA to AChE with affinities comparable to 10-40. The apparent discrepancy between gene expression and predicted inhibition may reflect analysis of whole-body homogenates, which include non-neuronal tissues [33]. Brain-specific studies are needed to clarify cholinergic effects. The stronger protective effects observed at 0.01-0.1 mM compared to higher doses suggest a hormetic or biphasic response, commonly reported for polyphenols, where low-to-moderate concentrations activate adaptive defense pathways without additional benefit at higher levels [34,35].

Overall, p-MCA exerts multi-target neuroprotective effects in *D. melanogaster* by enhancing antioxidant defenses, preserving mitochondrial function, modulating apoptosis, and interacting with cholinergic targets. The integration of *in vivo* and *in silico* analyses strengthens the mechanistic interpretation and supports the suitability of *Drosophila* for early-stage neuroprotective screening. However, translational limitations must be acknowledged. As an invertebrate model, *Drosophila* may not fully reflect vertebrate systems [36]. Furthermore, analyses were limited to gene expression in whole-body homogenates without protein-level validation, functional cellular assays, or histopathological evaluation [33,37,38]. Future studies should validate these findings in vertebrate models, including zebrafish or mammals, and incorporate protein-level, histological, and safety assessments to better establish the translational potential of p-MCA in AD.

Conclusions

This study demonstrates the neuroprotective potential of p-MCA against Alzheimer's disease (AD)-like pathology through multi-target mechanisms. In *D. melanogaster*, p-MCA improved survival, locomotor activity, and cognitive-related behavior following $AlCl_3$-induced neurotoxicity. Gene expression analyses indicated modulation of antioxidant, apoptosis-related, and aging-associated pathways, supporting enhanced cellular resilience under neurodegenerative stress. *In silico* docking showed strong binding affinity of p-MCA to acetylcholinesterase, comparable to 10-40,

suggesting potential cholinergic modulation. The divergence between AChE expression and predicted inhibition underscores the need for tissue-specific validation. Collectively, these integrated phenotypic, molecular, and computational findings support p-MCA as a potential multi-target neuroprotective candidate that warrants further preclinical and translational investigation.

Acknowledgements

The authors would like to express their sincere gratitude to Prof. Takayuki Kuraishi from Kanazawa University, Ishikawa 920-1192, Japan, for his invaluable support in providing the necessary materials and special consumables, particularly the wild-type strain of *D. melanogaster* used in this study. Furthermore, the authors extend their acknowledgments to Prof. Elly Wahyuddin (Biofarmaka Laboratory, Faculty of Pharmacy, Universitas Hasanuddin, Indonesia), for generously providing all the required instruments to carry out this research. This research was funded by the Directorate General of Higher Education, Ministry of Education, Culture, Research, and Technology, Indonesia, through the PDD 2024 research grant (Contract Number 027/E5/PG.02.00.PL/2024), awarded to B.J.L and colleagues.

Declaration of Generative AI in Scientific Writing

This study used artificial intelligence (AI) tools and methodologies in the following capacity: Manuscript Writing Support: AI-based language model ChatGPT was employed in the language refinement (improving grammar, sentence structure, and readability of the manuscript). We confirm that all AI-assisted processes were critically reviewed by the authors to ensure the integrity and reliability of the results. The final decisions and interpretations presented in this article were solely made by the authors.

CRediT Author Statement

Nur Rahma Rumata: Conceptualization; Methodology; Investigation; Formal analysis; Writing – Original draft preparation, Data curation. **Asbah Asbah:** Investigation; Formal analysis; Data curation; Validation. **Nadila Pratiwi Latada:** Investigation; Visualization; Data curation. **Muhammad Arfandy Gunawan:** Software; Formal analysis; Visualization. **Fifi Dismayanti Indriani Nainu:** Resources; Validation; Writing – Review & Editing. **Irmanida Batubara:** Methodology; Resources; Supervision. **Muhammad Aswad:** Project administration; Resources; Supervision. **Berry Juliandi:** Conceptualization; Supervision; Writing – Review & Editing; Funding acquisition. **Firzan Nainu:** Conceptualization; Methodology; Writing – Review & Editing; Supervision.

References

[1] J Guo, X Huang, L Dou, M Yan, T Shen, W Tang and J Li. Aging and aging-related diseases: From molecular mechanisms to interventions and treatments. *Signal Transduction and Targeted Therapy* 2022; **7**, 391.

[2] Y Li, X Tian, J Luo, T Bao, S Wang and X Wu. Molecular mechanisms of aging and anti-aging strategies. *Cell Communication and Signaling* 2024; **22**, 285.

[3] E Passeri, K Elkhoury, M Morsink, K Broersen, M Linder, A Tamayol, C Malaplate, FT Yen and E Arab-Tehrany. Alzheimer's disease: Treatment strategies and their limitations. *International Journal of Molecular Sciences* 2022; **23(22)**, 13954.

[4] DC Miculas, PA Negru, SG Bungau, T Behl, SSU Hassan and DM Tit. Pharmacotherapy evolution in Alzheimer's disease: Current framework and relevant directions. *Cells* 2023; **12(1)**, 131.

[5] JW Kinney, SM Bemiller, AS Murtishaw, AM Leisgang AM Salazar and BT Lamb. Inflammation as a central mechanism in Alzheimer's disease. *Alzheimer's & dementia* 2018; **4**, 575-590.

[6] Y Zhang, H Chen, R Li, K Sterling and W Song. Amyloid β-based therapy for Alzheimer's disease: Challenges, successes and future. *Signal Transduction and Targeted Therapy* 2023; **8**, 248.

[7] PT Kamatham, R Shukla, DK Khatri and LK Vora. Pathogenesis, diagnostics, and therapeutics for Alzheimer's disease: Breaking the memory barrier. *Ageing Research Reviews* 2024; **101**, 102481.

[8] E Hogervorst, E Schröder-Butterfill, YS Handajani, P Kreager and TB W Rahardjo. Dementia and dependency vs. proxy indicators of

the active ageing index in Indonesia. *International Journal of Environmental Research and Public Health* 2021; **18(16)**, 8235.

[9] J Zhang, Y Zhang, J Wang, Y Xia, J Zhang and L Chen. Recent advances in Alzheimer's disease: Mechanisms, clinical trials and new drug development strategies. *Signal Transduction and Targeted Therapy* 2024; **9**, 211.

[10] B Miziak, B Błaszczyk and SJ Czuczwar. Some candidate drugs for pharmacotherapy of Alzheimer's disease. *Pharmaceuticals* 2021; **14(5)**, 458.

[11] LK Huang, SP Chao and CJ Hu. Clinical trials of new drugs for Alzheimer disease. *Journal of Biomedical Science* 2020; **27**, 18.

[12] A Płowuszyńska and A Gliszczyńska. Recent developments in therapeutic and nutraceutical applications of *p-MCA* from plant origin. *Molecules* 2021; **26(13)**, 3827.

[13] T Begum, R Gogoi, N Sarma, SK Pandey and M Lal. Novel ethyl p-methoxy cinnamate rich *Kaempferia galanga* (L.) essential oil and its pharmacological applications: Special emphasis on anticholinesterase, anti-tyrosinase, α-amylase inhibitory, and genotoxic efficiencies. *PeerJ* 2023; **11**, 14606.

[14] A Finelli, A Kelkar, HJ Song, H Yang and M Konsolaki. A model for studying Alzheimer's Aβ42-induced toxicity in *D. melanogaster*. *Molecular and Cellular Neuroscience* 2004; **26(3)**, 365-375.

[15] UB Pandey and CD Nichols. Human disease models in *D. melanogaster* and the role of the fly in therapeutic drug discovery. *Pharmacological Reviews* 2011; **63(2)**, 411-436.

[16] H Bolus, K Crocker, G Boekhoff-Falk and S Chtarbanova. Modeling neurodegenerative disorders in *D. melanogaster*. *International Journal of Molecular Sciences* 2020; **21(9)**, 3055.

[17] LM Luheshi, GG Tartaglia, AC Brorsson, AP Pawar, IE Watson, F Chiti, M Vendruscolo, DA Lomas, CM Dobson and DC Crowther. Systematic *in vivo* analysis of the intrinsic determinants of amyloid β pathogenicity. *PLoS Biology* 2007; **5(11)**, 290.

[18] F Nainu, E Salim, RM Asri, A Hori and T Kuraishi. Neurodegenerative disorders and sterile inflammation: Lessons from a *Drosophila* model. *The Journal of Biochemistry* 2019; **166(3)**, 213-221.

[19] NR Rumata, D Purwaningsih, A Asbah, MF As'Ad, D Chadran, TB Emran and F Nainu. Phenotypical and molecular assessments on the pharmacological effects of curcumin in *D. melanogaster*. *Narra J* 2023; **3(2)**, 117.

[20] C Welch, E Johnson, A Tupikova, J Anderson, B Tinsley, J Newman, E Widman, A Alfareh, A Davis, L Rodriguez, C Visger, JP Miller-Schulze, W Lee and K Mulligan. Bisphenol a affects neurodevelopmental gene expression, cognitive function, and neuromuscular synaptic morphology in *D. melanogaster*. *Neurotoxicology* 2022; **89**, 67-78.

[21] LL Vang, AV Medvedev and J Adler. Simple ways to measure behavioral responses of *Drosophila* to stimuli and use of these methods to characterize a novel mutant. *PLoS One* 2012; **7(5)**, 37495.

[22] C Solana-Manrique, MD Moltó, P Calap-Quintana, FJ Sanz, JV Llorens and N Paricio. *Drosophila as a model system for the identification of pharmacological therapies in neurodegenerative diseases*. Springer, Singapore, 2019, p. 433-467.

[23] M Aswada, R Nugrahaa, R Yuliantya, Ismaila, YM Evarya, Kasmiatib and ZP Tachrimc. Potency of bisindoles from caulerpa racemosa in handling diabetes-related complications: *In silico* ADMET properties and molecular docking simulations. *Turkish Computational and Theoretical Chemistry* 2024; **8(3)**, 99-107.

[24] CDK Amengor, P Biniyam, AA Brobbey, FK Kekessie, FK Zoiku, S Hamidu, P Gyan and BM Abudey. N-substituted phenylhydrazones kill the ring stage of *Plasmodium falciparum*. *BioMed Research International* 2024; **2024**, 6697728.

[25] N Mert-Ozupek, G Calibasi-Kocal, N Olgun, Y Basbinar, L Cavas and H Ellidokuz. In-silico molecular interactions among the secondary metabolites of *Caulerpa* spp. and colorectal cancer targets. *Frontiers in Chemistry* 2022; **10**, 1046313.

[26] H Rasyid, NH Soekamto, S Firdausiah, R Mardiyanti, B Bahrun, Siswanto, M Aswad, WD Saputri, AAT Suma, NH Syahrir and RV

Listyarini. Revealing the potency of 1, 3, 5-Trisubstituted pyrazoline as antimalaria through combination of *in silico* studies. *Sains Malaysiana* 2023; **52(10)**, 2855-2867.

[27] A Drakontaeidi and E Pontiki. Multi-target-directed cinnamic acid hybrids targeting Alzheimer's disease. *International Journal of Molecular Sciences* 2024; **25(1)**, 582.

[28] J Xu, X Su, SK Burley and XFS Zheng. Nuclear SOD1 in growth control, oxidative stress response, amyotrophic lateral sclerosis, and cancer. *Antioxidants* 2022; **11(2)**, 427.

[29] A Houldsworth. Role of oxidative stress in neurodegenerative disorders: A review of reactive oxygen species and prevention by antioxidants. *Brain Communications* 2024; **6(1)**, 356.

[30] T Alqahtani, SL Deore, AA Kide, BA Shende, R Sharma, RD Chakole, LS Nemade, NK Kale, S Borah, SS Deokar, A Behera, DD Bhandari, N Gaikwad, AK Azad and A Ghosh. Mitochondrial dysfunction and oxidative stress in Alzheimer's disease, and Parkinson's disease, Huntington's disease and amyotrophic lateral sclerosis-an updated review. *Mitochondrion* 2023; **71**, 83-92.

[31] S Tripathi and S Sinha. Small heat shock protein and *D. melanogaster* development. *Advances in Zoology and Botany* 2023; **11(4)**, 246-256.

[32] CJ Sproston, JE Rak, EC Marin, S Kondo and DW Williams. Hemilineage-specific deployment of the pro-apoptotic RHG genes *reaper* and *grim* during neurogenesis sculpts segment and sex-specific neural network composition in *Drosophila*. *Development* 2025; **152(21)**, dev204902.

[33] OB Ogunsuyi, OC Olagoke, BA Afolabi, G Oboh, OM Ijomone, NV Barbosa and JBT da Rocha. Dietary inclusions of Solanum vegetables mitigate aluminum-induced redox and inflammation-related neurotoxicity in *D. melanogaster* model. *Nutritional Neuroscience* 2022; **25(10)**, 2077-2091.

[34] EJ Calabrese, P Pressman, AW Hayes, G Dhawan, R Kapoor, E Agathokleous, LA Baldwin and V Calabrese. The chemoprotective hormetic effects of rosmarinic acid. *Open Medicine* 2024; **19(1)**, 20241065.

[35] P Perrone and S D'Angelo. Hormesis and health: Molecular mechanisms and the key role of polyphenols. *Food Chemistry Advances* 2025; **7**, 101030.

[36] Y Liu. Zebrafish as a model organism for studying pathologic mechanisms of neurodegenerative diseases and other neural disorders. *Cellular and Molecular Neurobiology* 2023; **43**, 2603-2620.

[37] A Samih, MADM Ferreira and Z Nikoloski. Gene expression and protein abundance: Just how associated are these molecular traits? *Biotechnology Advances* 2026; **86**, 108720.

[38] N Dhiman, S Deshwal, R Vikas, NK Singhal and S Rajat. Zebrafish as a model organism to study sporadic Alzheimer's disease: Behavioural, biochemical and histological validation. *Experimental Neurology* 2025; **383**, 115034.